

Ali K. Muftah¹

Department of Mechanical Engineering,
Sabratra University,
University Avenue 100,
Sabratra, Libya
e-mail: ali.muftah@sabu.edu.ly

Hacen Dhahri

National Engineering School,
Monastir University,
Thermal and Energetic Systems Studies
Laboratory,
Rue Ibn Jazzar,
Monastir 5019, Tunisia
e-mail: hassen.dhahri@enim.u-monastir.tn

Leila Zili-Ghedira

National Engineering School,
Monastir University,
Thermal and Energetic Systems Studies
Laboratory,
Rue Ibn Jazzar,
Monastir 5019, Tunisia
e-mail: leila.zili@enim.u-monastir.tn

Mabruk M. Abugderah

Research and Consultation Centre, SABU,
University Avenue 100, P.O. Box 250,
Sabratra 00218, Libya
e-mail: mabrouk@sabu.edu.ly

Mathematical Modeling and Simulation of Multi-Effect Distillation Without Thermal Vapor Compressor Applied to Zuara Desalination Plant

Mathematical thermodynamic modeling is used in desalination systems to obtain unknown values and predict various properties such as enthalpy or phase equilibrium. These models are useful to understand system behavior. A mathematical modeling of a multi-effect distillation (MED) plant without a thermal vapor compressor (TVC) was performed to simulate and forecast the temperatures, mass flowrates, and the productivity of each cell of steam. The total productivity of the desalination unit and the performance rate in different operating conditions were also found. A PYTHON program was used to solve the model equations. The evaluation indicates that the model is reliable and its predictions matched well with the real data obtained from Zuara desalination plant. This subject was selected for research because most studies concentrate on MED with TVC or MED of low cell number and without TVC. The obtained results show that the productivity of the system and the gain output ratio are directly proportional to seawater temperature and inversely proportional to plant load. The model can be utilized to estimate the performance of desalination plants of MED without TVC. The model was validated using industrial data.

[DOI: 10.1115/1.4051452]

Keywords: desalination, multi-effect, mathematical modeling, GOR, condensation, energy systems, evaporation, heat and mass transfer, low-temperature heat transfer, thermal systems

1 Introduction

Water is the main requisite for any prosperous life and development [1]. The main part of freshwater is stored in the Arctic and Antarctic ice sheets. Our land is rich in water, but unfortunately, only a small part (about 0.3%) is drinkable and suitable for human use. The other 99.7% are found in oceans, soil, and ice, floating in the atmosphere, and essentially unattainable [2,3]. Water scarcity appeared because of the massive growth in population, living standards, and the rapid development of the agricultural and industrial sectors [4].

Desalination is an alternative and beneficial method to provide a solution for the acute shortage of drinking water. After decades of development, the global cumulative contracted capacity of desalination has reached $9.74 \times 10^7 \text{ m}^3/\text{d}$ by 2018 and more than 20,000 desalination plants had been constructed around the world [5]. However, the cost of producing water through various techniques of desalination is still expensive due to energy consumption [6].

The desalination or separation of freshwater from seawater is a thermodynamic process that requires a high amount of energy [7]. It is classified as one of the most energy-intensive water supply and treatment processes [8]. The energy required for the desalination process depends on several factors such as the type of used technology plant design, temperature, and quality of the feed water, as well as the extent to which energy recovery devices are used or the quality required for the produced water [2,9,10].

In common, there are two main types of seawater desalination technologies; one is the membrane or processes without phase change, and the other is thermal or phase change processes [11].

Desalination thermal processes are generally found in countries, where fuel is relatively cheap and steam is invoked as the working fluid in desalination thermal type. The membrane process functions similar to mechanical strainers where water particles permeate through a semi-permeable membrane to produce permeate with little dissolved elements [12,13].

Reverse osmosis (RO) desalination is the most widely applied method accounting for 65%, followed by multi-stage flash (MSF) desalination, multi-effect distillation (MED), and other methods with 22%, 8%, and 5%, respectively [2,14]. In Libya, there are currently about 21 operating desalination plants, with a total capacity of 525, 680.00 m^3/d . Thermal processes represent about 95% of the operable desalination plants, while RO technology represents about 5% [15].

The total specific energy consumption (thermal/electricity) in MED and MSF is 5.5–9 kW/m^3 and 10–16 kW/m^3 , respectively [16]. MED electricity consumption is between 1.5 and 2.5 kWh/m^3 , which is lower than those of the MSF and SWRO desalination technologies with electricity consumption of 2–4 kWh/m^3 and 3–4 kWh/m^3 , respectively [14]. The MED has some unique advantages over the other two methods. The corrosion and expandability of the equipment are effectively controlled because the temperature of the upper brine in MED (no more than 70 °C) is much lower than that of MSF (90–110 °C). Also, there is a simpler treatment for seawater feed with chemicals with lower consumption and higher product water quality than RO [17]. In addition, the high flexibility and low operating temperature of the MED system make this possible to be integrated with industrial processes to recover heat waste and the potential to use renewable energy [18].

Many desalination processes have been developed, but not all are reliable and in commercial use, and most of the extensive research in the field of desalination focus on improving the performance in order to achieve a reduction in the production cost per cubic

¹Corresponding author.

Manuscript received February 28, 2021; final manuscript received June 1, 2021; published online August 3, 2021. Assoc. Editor: Stephen A. Solovitz.

meter of desalinated water [19]. Hatzikioseyan et al. [20] carried out a study about modeling and thermodynamic analysis of a multi-effect distillation plant installed in a PSA (Almeria Solar Platform). The plant has been used as a pilot unit for seawater desalination in various European research projects. The authors developed and improved a modeling and simulation program based on the plant design criteria. The model relied on the mass and energy balances of the currents flow during each stage of the distillate unit to predict unit performance in terms of energy requirements.

Ameri et al. [21] studied the effects of various design parameters on MED system specifications. They showed the existence of an optimum value depending on the salinity of seawater and influence the temperature difference and the temperature of the feed water. Again, they showed that large values of the inlet vapor pressure improve the performance ratio and the required heat transfer surface area of the system and reduces the cooling seawater mass flowrate.

Abdul-Wahab et al. [22] introduced a mathematical model for multi-stage flash (MSF) desalination plants. For each stage, the developed model was used to predict the temperatures of brine, distillate, and cooling brine, and the flowrates of brine outlet and distillate production. The developed model was evaluated with the MSF plant vendor simulation results and its actual operating data. The evaluation indicated that model predictions matched well with the vendor simulation results and the plant operating data. They recommended for determining the optimum set point of a running MSF desalination plant at different loads to maximize water production or minimize energy consumption.

A numerical study of steam parameters on the performance of a Thermal Vapor Compression-Multi-Effect Distillation plant using a commercial MED-thermal vapor compressor (TVC) was presented by Shen et al. [23]. It also presented the performance calculation of the MED-TVC desalination system with different steam pressures and temperatures. With higher steam pressure, the gained output ratio (GOR) of the desalination plant could get higher values. The recirculation position of vapor in a multi-effect distillation system has a great effect on the GOR as well.

A steady-state mathematical model of the MED-TVC system and its solution procedure was presented by Al-Mutaz et al. [24]. This study was developed based on the basic laws of material and energy balances and heat transfer equations with correlations for physical properties estimation. The influence of important design and operating variables on the performance of the plant was investigated. This study shows that the simulation model is an effective tool to design a MED-TVC system for a different number of effects with any desired capacity. In addition, it provides an effective tool to evaluate the system performance of any MED-TVC unit.

Zhou et al. [25] published a detailed mathematical model of multi-effect evaporation/multi-effect with thermal vapor compression is developed based on the first and second law of thermodynamics. Performance comparison between multi-effect evaporation and that with thermal vapor compression was accomplished from the perspective of exergy destruction as well. Results show that a higher gained output ratio and lower specific cooling water can be acquired when the compression ratio of the thermal vapor compressor is 2.1–2.6.

A performance study of a pilot-scale low-temperature multi-effects desalination plant is presented by Qi et al. [26]. The results provide a useful reference for the design of other large-scale seawater desalination systems. A paper published by Gao et al. [27] considered the effects of boiling point elevation (BPE), the influence of heat loss of condenser tubes, the unequal temperature drops in each flash stage, and the effect of the reject seawater recycle mass flowrate. The study results can be used for guidelines of real-time optimization of the MSF system.

Zhou et al. [28] realized a work that deals with the feed configurations suitable for the large-scale LT-MED desalination plant based on a reasonable spray density, which includes the parallel feed and mixed feed. The validity of the established model was verified through comparison with the industrial data. The comparison

of performance and scaling tendencies among various feed configurations was accomplished. The authors showed that the mixed feed system presents a better performance than the parallel feed systems, while the scaling risk of the combination of backward and parallel feed configuration is the highest. This comparison illustrates the logic behind choosing each feed configuration.

Guo et al. [29] developed a mathematical model for a five-effect forward SE-MED system with a bleed fraction of 20%. Their results show that a high evaporation efficiency of 99.86% is achievable by the modified SET. A review study on the scope and extent of development of mathematical models used for the forward feeding multi-effect distillation process was presented by Al-Hotmani et al. [30]. It highlights the advantages and disadvantages of such models. Liu et al. [31] introduced the evaporator structural design (ESD) model. The multi-effect evaporation (MEE) forward feed station was calculated with 14 effects using an ESD model. According to the authors, the relative error of the accumulated vapor mass flowrate in each effect ranged between 1% and 8%, and the evaporator area ratio is about 7%.

Muftah [32] published an article about the possibility of replacing the de-superheating steam system with a steam turbine for the Zuara desalination plant. The results showed that 11.9 MW of electricity could be produced. The cost of a cubic meter of produced water can be reduced by 12%. El-Helw et al. [33] proposed a new design for solar-powered desalination plants including the solar parabolic collectors, the steam generator, and the MED unit for transporting the conventional plant. They showed that THERMINOL VP1 contained 1.025% more desalinated water than the other species. In addition, the operation cost of the distillate production by the usage of conventional fuel is much more than solar energy.

Most modeled desalination plants in the literature were conducted for MED with TVC or for MED without TVC and small number of cells. The novelty of this study is that it models a MED plant with any number of cells and without TVC. Zuara desalination plant is unique because it is the only MED working without TVC in Libya. It is located in Zuara, 100 km west of Tripoli. It was constructed in two stages. The first one is a multi-effect evaporation without vapor compressor (MED) with three total units' capacity of 40,000 m³/d. The production of this stage was started in March 2006. The second stage, which depends on multi-effect with thermal compressor (MED-TVC), has two units' capacity of 40,000 m³/day. Both stages were supplied and constructed by SIDEM, a French company.

Over time, and due to the operating conditions of the plant, there was a decrease in the productivity of steam boilers in the first stage, which led to the final suspension of this stage by the end of 2014 to make the necessary maintenance of the boilers [34].

This study covers the first stage of the plant (Fig. 1), which consists of three evaporators. Each one has a capacity of 13,334.00 m³/day (556.00 m³/h), and it aims to develop a mathematical model able to simulate the thermal components of the plant such as temperature distribution and flowrates across all cells, preheaters, and condenser in the desalination unit. The aim is to predict the productivity and efficiency of the plant under different operating conditions and to determine the optimum operating mode for the plant. This model can be used to estimate the performance of MED without TVC.

2 Mathematical Modeling

Zuara desalination plant consists of seawater intake, evaporators, boilers, and potabilization unit. The evaporator as shown in Fig. 1 consists of nine isolated cells, eight feed water preheaters, a final condenser, and pumps to circulate distilled water, seawater, and brine from and to the desalination unit.

A steady-state mathematical model of MED and without TVC system and its solution procedure is presented in this section. The process is considered to be adiabatic due to insulation and low operational temperature. The salt concentration in the distillate and vapor is considered to be zero. According to the law of mass

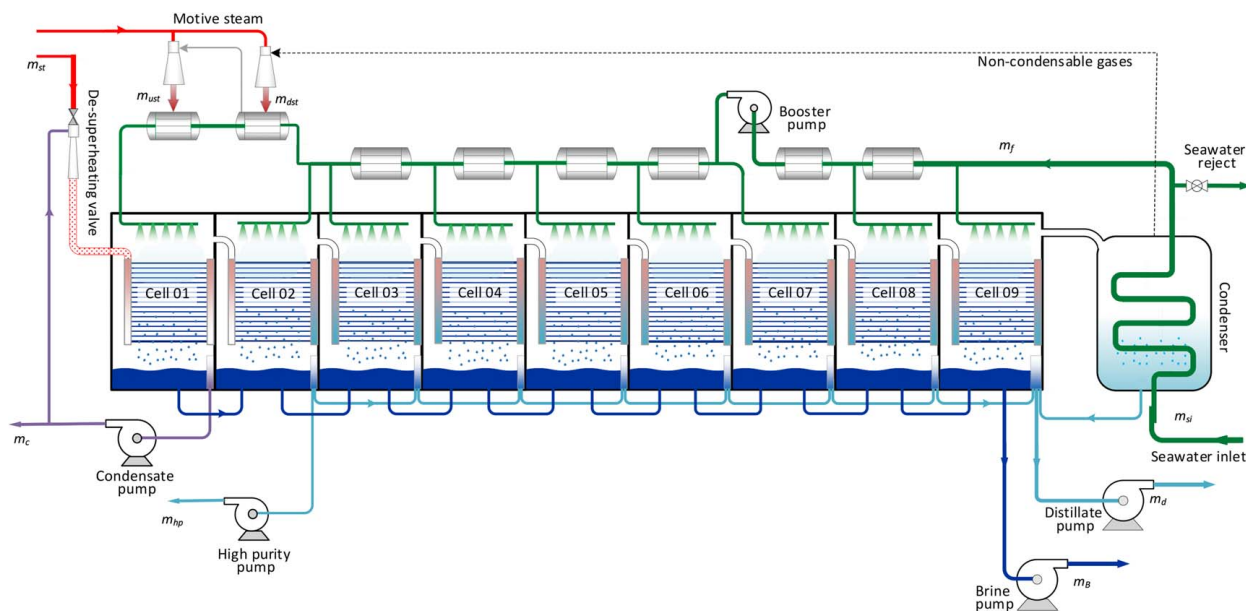


Fig. 1 Schematic diagram of the plant evaporator

conservation, the mass of the reactants, in a steady-state and steady flow process, must be equal to the mass of the products. Energy balance or thermal balance can be inferred directly from the first law of thermodynamics.

The external preheaters exist in order to heat up the feed flow to evaporation temperature. Hence, the terminal temperature difference and the BPE are bridged [2].

Mass balance or calculating materials entering and exiting the system can identify mass flows that may be unknown or difficult to measure. Figures 2 and 3 show all inlet and outlet system streams.

The steam coming from the boiler at high pressure and temperature passes through a de-superheating valve in which a measured quantity of water is injected. The steam, in this case, is turned into its saturated state at a temperature and pressure that suits the evaporator needs (Fig. 2). Applying the conservation of mass and energy on the de-superheating valve, the following equation is obtained:

$$\dot{m}_{st} + \dot{m}_{c1} = \dot{m}_{st1} \quad (1)$$

$$\dot{m}_{st} \times h_{st} + \dot{m}_{st1} \times h_{st1} = \dot{m}_{c1} \times h_{c1} \quad (2)$$

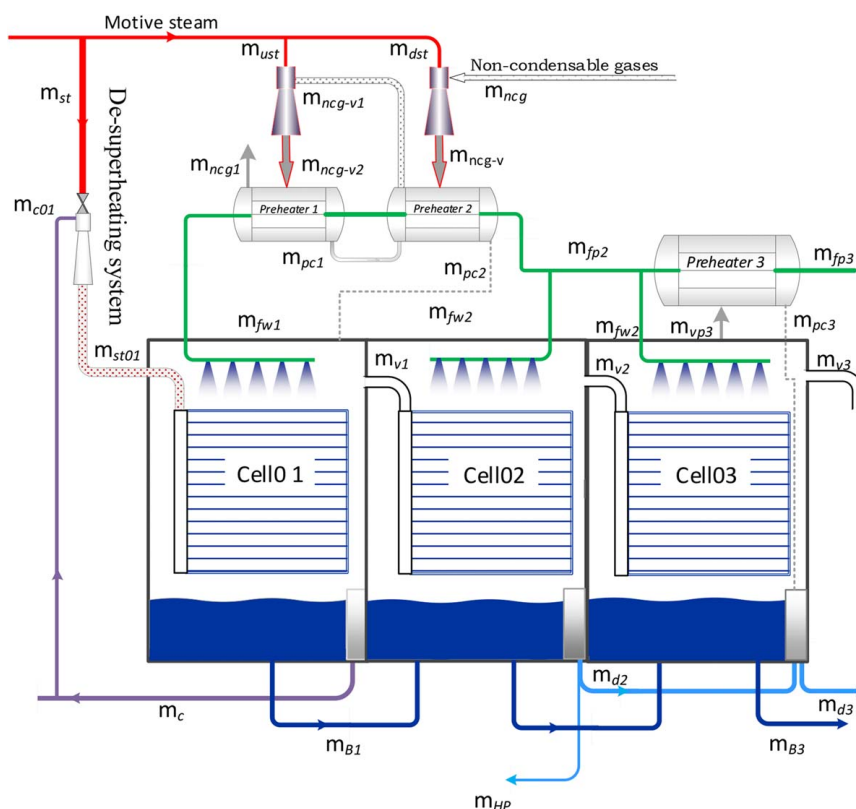


Fig. 2 Mass and thermal balances diagram of the hot end evaporator

The mass balance for the middle cells is given by the following equation:

$$\dot{m}_{v(j-1)} + \dot{m}_{fwj} + \dot{m}_{B(j-1)} + \dot{m}_{d(j-1)} + \dot{m}_{PCj} = \dot{m}_{dj} + \dot{m}_{Bj} + \dot{m}_{vj} + \dot{m}_{Pvj} \quad \text{for } j = 4 \text{ to } 8 \quad (18)$$

The mass balance for the last cell is as follows:

$$\dot{m}_{v8} + \dot{m}_{fw9} + \dot{m}_{B8} + \dot{m}_{d8} + \dot{m}_{PC9} + \dot{m}_{d9} = \dot{m}_d + \dot{m}_B + \dot{m}_{v9} + \dot{m}_{Pv9} \quad (19)$$

where \dot{m}_d is the unit total distillate water produced and \dot{m}_B is the total brine unit outlet.

The energy balance of all cells is given by

$$\dot{Q}_{st1} + \dot{Q}_{fw1} = \dot{Q}_C + \dot{Q}_{B1} + \dot{Q}_{v1} \quad (20)$$

$$\dot{Q}_{fw2} + \dot{Q}_{v1} + \dot{Q}_{B1} = \dot{Q}_{d2} + \dot{Q}_{B2} + \dot{Q}_{v2} \quad (21)$$

$$\dot{Q}_{v2} + \dot{Q}_{fw3} + \dot{Q}_{B2} + \dot{Q}_{d2} - \dot{Q}_{HP} + \dot{Q}_{PC3} = \dot{Q}_{d3} + \dot{Q}_{B3} + \dot{Q}_{v3} + \dot{Q}_{Pv3} \quad (22)$$

$$\dot{Q}_{v(j-1)} + \dot{Q}_{fwj} + \dot{Q}_{B(j-1)} + \dot{Q}_{d(j-1)} + \dot{Q}_{PCj} = \dot{Q}_{dj} + \dot{Q}_{Bj} + \dot{Q}_{vj} + \dot{Q}_{Pvj} \quad \text{for } j = 4 \text{ to } 8 \quad (23)$$

$$\dot{Q}_{v8} + \dot{Q}_{fw9} + \dot{Q}_{B8} + \dot{Q}_{d8} + \dot{Q}_{PC9} + \dot{Q}_{d9} = \dot{Q}_d + \dot{Q}_B + \dot{Q}_{v9} + \dot{Q}_{Pv9} \quad (24)$$

where the heat rate is stated as follows:

$$\dot{Q}_{mn} = \dot{m}_{mn} \times h_{mn} \quad (25)$$

and m denotes the stream type and n indicates the cell or preheater number.

One of the important parameters that need to be obtained is brine salinity. It is calculated as follows:

$$\dot{m}_{fw1} \times S_{fw} = \dot{m}_{B1} \times S_{B1} \quad (26)$$

$$\dot{m}_{fwj} \times S_{fw} + \dot{m}_{B(j-1)} \times S_{B(j-1)} = \dot{m}_{Bj} \times S_{Bj} \quad \text{for } j = 2 \text{ to } 8 \quad (27)$$

$$\dot{m}_{fw9} \times S_{fw} + \dot{m}_{B8} \times S_{B8} = \dot{m}_B \times S_B \quad (28)$$

The salinity of vapor, condensate, and distilled water is assumed to be equal to zero.

The last component in the MED desalination plant is the condenser (Fig. 3). It works as a heat exchanger to condense the vapor produced in the last cell using seawater as the cooling medium. The vacuum system is connected to the condenser to remove the non-condensable gases and keep the evaporator under excessive vacuum.

Considering the inlet and outlet condenser flow streams the mass and energy balances are given by:

$$\dot{m}_{v9} + \dot{m}_{sw} = \dot{m}_{d9} + \dot{m}_{sw} + \dot{m}_{ncg} \quad (29)$$

where \dot{m}_{sw} is the total mass flowrate inlet seawater inlet the condenser.

$$\dot{m}_{v9} \times h_{v9} + \dot{m}_{sw} \times h_{swi} = \dot{m}_{d9} \times h_{d9} + \dot{m}_{sw} \times h_{swe} + \dot{m}_{ncg} \times h_{ncg} \quad (30)$$

2.1 Gain Output Ratio. The gain output ratio is defined as the mass of produced freshwater divided by the mass of steam used to produce this freshwater. Therefore, it is a measure of the thermal efficiency of the distillation plant. It can be calculated using the following formula [35]:

$$GOR = \frac{\dot{m}_{td}}{\dot{m}_{st}} \quad (31)$$

where \dot{m}_{td} is the total produced desalinated water (t/h) and \dot{m}_{st} is the consumed operational steam (t/h).

2.2 Specific Heat Transfer Area. Specific heat transfer area (SHTA) is the ratio of the heat transfer area (HTA) to the produced desalinated water (\dot{m}_{td}). It is considered as a criterion for equipment cost evaluation. It can be calculated using the equation [25]:

$$SHTA = \frac{A}{\dot{m}_{td}} = \frac{\sum_{i=1}^n A_i + \sum_{j=1}^m A_{prej} + A_{con}}{\dot{m}_{td}} \quad \text{m}^2/(\text{kg/s}) \quad (32)$$

where A_i , A_{prej} , and A_{con} are the heat transfer area of the cell i , feed water preheater j , and condenser, respectively, and \dot{m}_{td} is the total predicted distillate water mass flowrate (Kg/s).

3 Plant Design Data

The study was conducted using design data obtained from the plant catalog (Table 1).

Make-up flowrate is directly linked to the production flowrate and seawater salinity and should be selected to keep the good wetting rate of the cell tube bundle to avoid scaling. It can be estimated from the recovery rate φ by [2]

$$\varphi = \frac{\dot{m}_d}{\dot{m}_f} = 1 - \frac{1}{CF} \quad (33)$$

where CF is the concentration factor, \dot{m}_d and \dot{m}_f are mass flowrates of distillate water and feed water makeup (t/h), respectively.

Reject and last cell temperatures depend on the project. To avoid scaling the maximum outlet temperature is normally kept below 50 °C. It is usually chosen to be 10 °C above the summer seawater temperature. On the other hand, top brine temperature is generally recommended not to exceed 65 °C in permanent conditions [2]. This value may be exceeded for given periods, providing particular care has to be taken for the anti-scale injection.

The temperature difference is necessary to have a driving force for the flash evaporation in each stage. It is given by the equation:

$$\Delta T_{stage} = \frac{\Delta T_o}{N} \quad (34)$$

where the overall temperature difference (ΔT_o) is equal to the difference between top brine and last cell brine temperatures.

High purity water is taken from the second cell distillate water which has lower conductivity than the distillate water produced by the other cells. It is used for boiler working fluid makeup to compensate the losses of the steam consumed as motive steam in the ejectors and heavy fuel heating in the combustion process.

4 Results and Discussion

The mathematical model was validated using real data obtained from the plant. Figure 4 shows the relationship between cell number and cell temperature, cell feed water temperature, and

Table 1 Desalination plant design data

Item	Symbol	Data value	Unit
Recovery rate	Φ	0.29	—
Concentration factor	CF	1.43	—
Makeup mass flow rate	\dot{m}_f	1836	t/h
Top brine temperature	T_{TBT}	70	°C
Seawater inlet temperature	T_{sw}	14–27	°C
Seawater salinity	S_{sw}	38,000	ppm
Stage temperature difference	ΔT_{stage}	3.7	°C
High purity water mass flowrate	\dot{m}_{HP}	5.0	t/h
Total heat transfer area	A	44,987.9	m ²

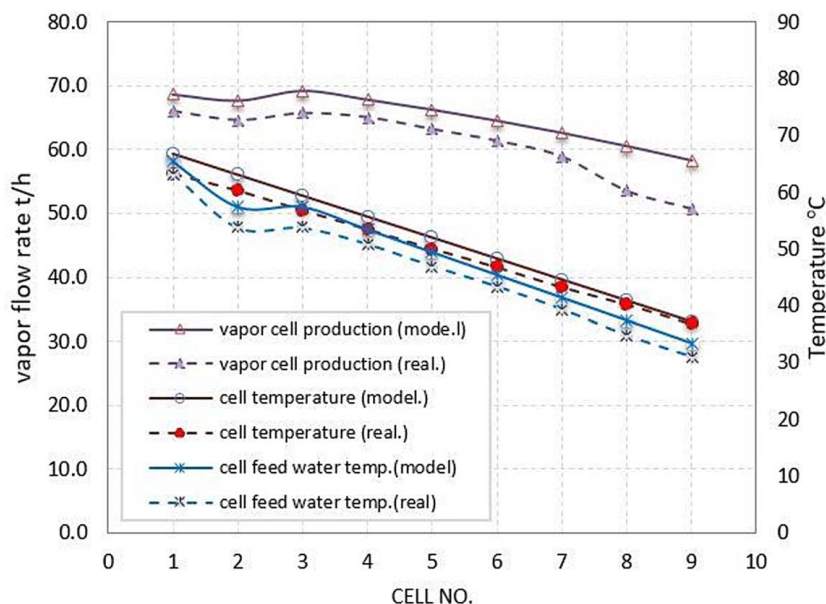


Fig. 4 Comparison between real and model results

Table 2 Vapor, distillate, and brine water produced from each stage at 27 °C

Cell no	Cell temp., °C	Feed water temperature, °C	Vapor outlet, t/h	Distillate outlet, t/h	Brine outlet, t/h
Cell 01	70.00	66.60	68.87	0.00	135.13
Cell 02	66.30	62.90	67.36	71.39	271.77
Cell 03	62.60	59.20	68.42	136.97	407.35
Cell 04	58.90	55.50	66.93	206.64	544.42
Cell 05	55.20	51.80	65.48	274.82	682.94
Cell 06	51.50	48.10	64.05	341.53	822.89
Cell 07	47.80	44.40	62.65	406.80	964.25
Cell 08	44.10	40.70	61.27	470.66	1106.98
Cell 09	40.40	37.00	59.91	580.48	1251.07

vapor cell production. As can be noted the real and model results have the same trend. It is worth mentioning that the Zuara desalination plant is the only MED without TVC in Libya, and no studies of a plant with a similar number of cells were found in the literature.

The design values are used in the mentioned mathematical model and the following results were obtained: Table 2 presents the produced vapor, distillate, and brine water from each stage at a sea-water inlet temperature of 27 °C. It is evident from Table 2 that the temperature of the cells decreases from the first cell in the direction of the ninth cell because the entry of the heat source is the first cell, and therefore, the heat is lost along the process.

The amount of vapor produced from cells decreases with the temperature of the cell, although the amount of feed water is constant in all cells. The mentioned decrease in the produced steam is due to the low temperature of the feed water, as it is known that the amount of evaporation is directly proportional to the water temperature (Fig. 5).

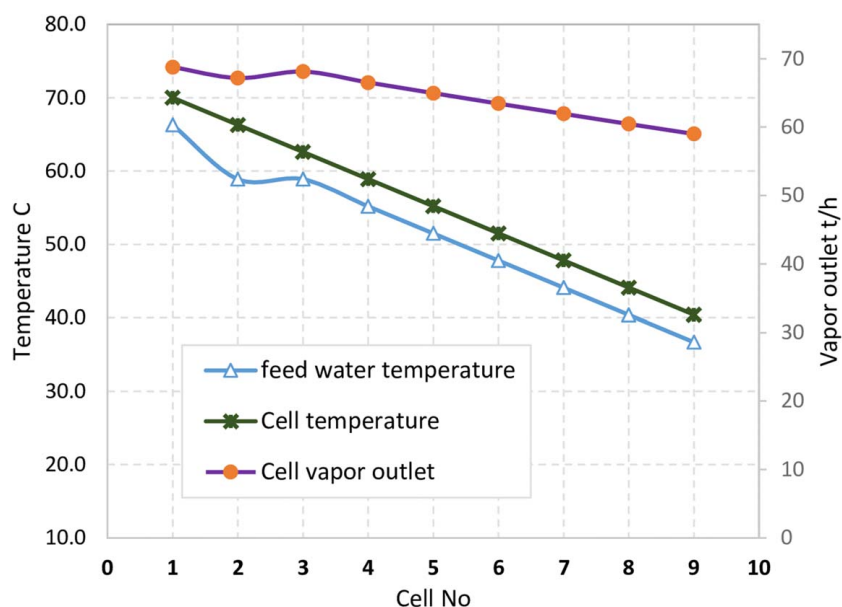


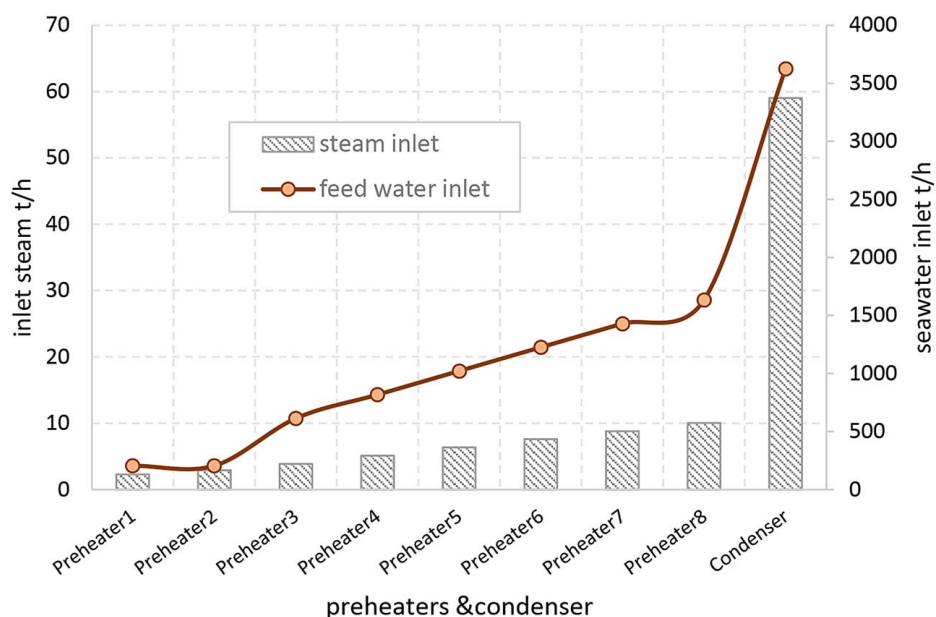
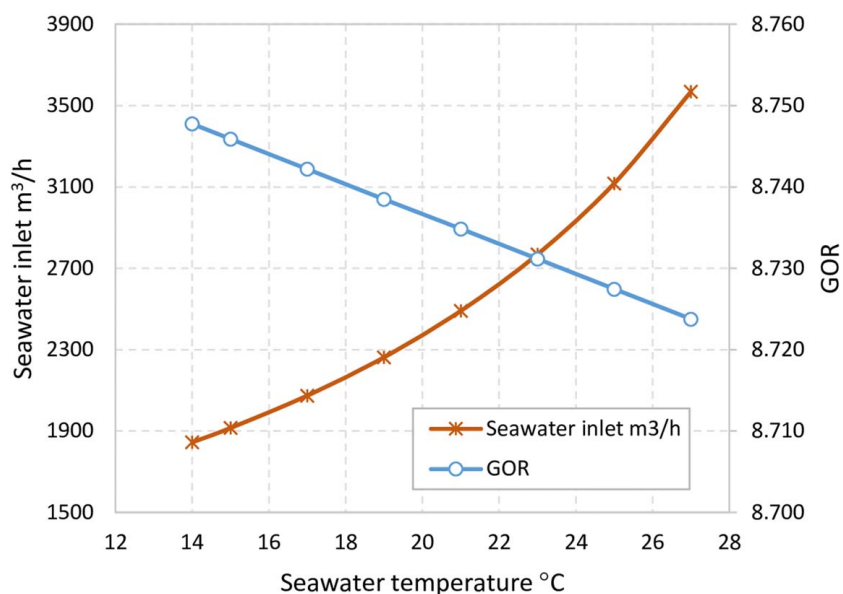
Fig. 5 cell vapor relationship

Table 3 Preheaters stream temperatures and mass flowrates

Preheater no	Seawater inlet Temperature, °C	Seawater outlet Temperature, °C	Seawater mass flow rate, t/h	Vapor mass flow rate, t/h
1	62.90	66.60	204.0	2.29
2	59.20	62.90	204.0	2.89
3	55.50	59.20	612.0	3.84
4	51.80	55.50	816.0	5.10
5	48.10	51.80	1020.0	6.35
6	44.40	48.10	1224.0	7.58
7	40.70	44.40	1428.0	8.81
8	37.00	40.70	1632.0	10.02
Condenser	27.00	37.00	3568.83	59.91

Table 4 Relationship between the seawater inlet temperature and unit performance

Seawater temperature °C	Distillate water mass flowrate \dot{m}_{td} , t/h	Seawater inlet mass flowrate \dot{m}_{sw} , t/h	Steam inlet mass flowrate \dot{m}_{st} , t/h	SHTA $m^2/(kg/s)$	GOR
14	582.035	1836.000	64.00	278.259	8.747
15	581.953	1915.360	64.00	278.298	8.746
17	581.706	2074.402	64.00	278.416	8.742
19	581.459	2262.724	64.00	278.535	8.738
21	581.217	2491.05	64.00	278.651	8.735
23	580.971	2769.132	64.00	278.769	8.731
25	580.725	3118.058	64.00	278.887	8.727
27	580.479	3568.828	64.00	279.005	8.724

**Fig. 6 Feed water and inlet steam flowrates****Fig. 7 Comparison between seawater inlet mass flowrate and GOR**

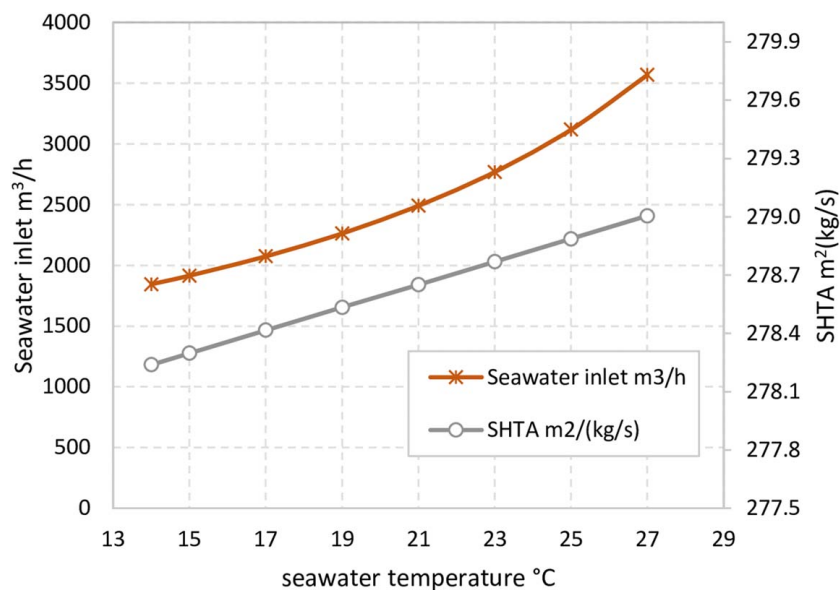


Fig. 8 The effect of seawater inlet temperature on unit productivity and SHTA

It is also noticed from the figure that the amount of steam produced in the second cell is low compared to the third cell due to the absence of a water preheater for the second cell (Fig. 2).

Table 3 presents the preheaters stream temperatures and mass flowrates. The first column shows the feed water inlet temperature, which ranges from 62.9 °C in the first preheater and 27 °C in the condenser inlet.

The amount of steam required to heat the feed water increases with the increase in the feed water flowrates, even though, the difference between the inlet and outlet temperatures of all preheaters is constant. However, the difference between the inlet and outlet condenser temperatures is high because of the high condenser inlet flowrates of the seawater and inlet steam from the last cell. The high amount of seawater flowrate is to make a sufficient cooling and to ensure the condensation of the steam inside the condenser as shown in Fig. 6.

Table 4 shows the relationship between the seawater inlet temperature and the flow rates of the distilled water, seawater inlet, unit steam inlet, the SHTA and the gain output ratio. In addition,

the latter is an indicator of the unit efficiency as it is inversely proportional to the seawater temperature, because of the need to increase the seawater flow rate during high ambient temperatures such as the summer season to ensure the necessary cooling and condensation of the final condenser.

Figure 7 demonstrates a comparison between seawater inlet mass flowrate and GOR. It can be seen, the relationship is inversely proportional to the gain output ratio and the seawater inlet temperature. Similarly, the flowrate of seawater is directly proportional to its temperature to ensure the condensation of the steam produced from the last cell and the rejected excess seawater to the ocean.

Figure 8 shows the effect of the seawater inlet temperature on the SHTA, which increases slightly with the increase in the seawater temperature due to the increase in the rate of seawater flow at the condenser necessary for cooling and the completion of the condensation process of the produced steam in the last cell. Since the total amount of feed water for all cells is constant at 1836 t/h, the excess seawater is rejected, which will carry with it an amount of heat as waste to the ocean.

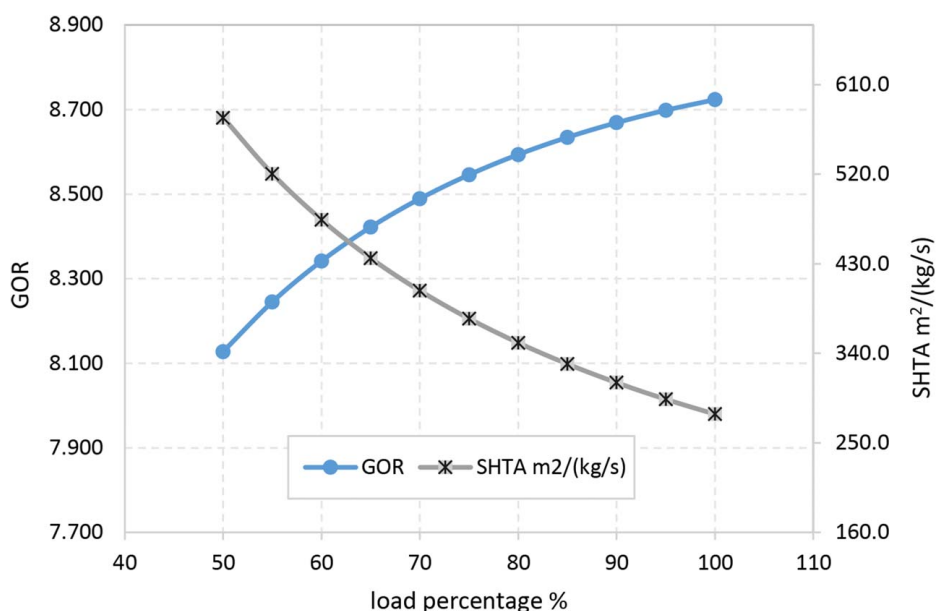


Fig. 9 Effect of load percentage on GOR and SHTA

Table 5 Effect of unit load percentage on the unit productivity and efficiency

Load percentage	Steam inlet, \dot{m}_{st} , t/h	Distillate water, \dot{m}_{dt} , t/h	GOR	SHTA, m ² / (kg/s)
50	32.0	280.725	8.128	576.922
55	35.2	311.171	8.245	520.474
60	38.4	341.513	8.342	474.232
65	41.6	371.750	8.422	435.659
70	44.8	401.883	8.489	402.994
75	48.0	431.912	8.546	374.976
80	51.2	461.835	8.594	350.680
85	54.4	491.654	8.635	329.411
90	57.6	521.368	8.669	310.638
95	60.8	550.976	8.699	293.945
100	64.0	580.479	8.724	279.005

Table 5 presents the relationship between the load percentage and the gain output ratio and the specific heat transfer area. As can be noted the GOR is directly proportional to the load percentage. For example, when the unit load rate changes from 50% to 100%, the unit gain output ratio increases by 7.212%. On the other hand, decreasing the percentage of the load decreases the produced distillate water as well as the gain output ratio of the desalination plant. This is due to the cell low temperature and the poor heating of the feed mass flowrate. The feed water flowrate is constant at each stage (Fig. 9).

The specific heat transfer area SHTA is inversely proportional to the load as shown in Fig. 8. This is due to the increase in distillate water product with load and keeping the heat transfer constant.

5 Conclusion

The mathematical equations related to the mass and energy balances of the thermal components of the Zuara desalination plant were modeled using plant design data. PYTHON computer program was used to solve the mathematical equations. Through this study, the utility of modeling and simulating desalination units becomes evident, in which the temperatures and flowrates are determined for all streams. Moreover, predicting the productivity of the plant under different operating conditions showed that the seawater temperature has an effect on the distilled water productivity and performance efficiency. They are also affected and directly proportional to the loading rate.

Through this study, the usefulness of modeling and simulation of desalination units is evident, where temperatures and flowrates are determined for all streams. Moreover, predicting the productivity of the plant under different operating conditions as the results showed that the seawater temperature affects the distilled water productivity and performance efficiency. In addition, the reduction of unit operation load affects the decrease in the gain output ratio by 7.21% and the increase in SHTA by 51.63%.

Acknowledgment

We would like to express our sincere thanks toward Zuara Desalination Plant engineers and staff for their valuable support in the implementation of this work.

Conflict of Interest

There are no conflicts of interest.

Data Availability Statement

The datasets generated and supporting the findings of this article are obtainable from the corresponding author upon reasonable

request. The authors attest that all data for this study are included in the paper.

Nomenclature

c	= condensate
d	= distillate
f	= make up water (feed water)
h	= stream enthalpy (kJ/kg)
\dot{m}	= stream mass flowrate (kg/s)
A	= heat transfer area (m ²)
B	= brine
I	= stream inlet
O	= stream outlet
P	= pressure (kPa)
\dot{Q}	= heat rate (kW)
S	= stream salinity percentage (ppm)
T	= temperature (°C)
V	= vapor
U_{st}	= upstream ejector motive steam
ΔT	= Temperature difference (°C)
ϕ	= recovery rate
D_{st}	= downstream ejector motive steam
F_p	= preheater feed water
F_w	= cell feed water
HP	= high purity water
ncg	= non-condensable gases
$ncg-v$	= mixture of non-condensable gases and vapor
P_c	= preheater condensate water outlet
P_v	= preheater vapor inlet
St	= steam
Sw	= seawater
Td	= total distillate

References

- [1] Najjar, Y., "Energy and Water Interdependence and Integration of Systems 2019," J. Environ. Soil Sci., <http://lupinepublishers.com/environmental-soil-science-journal/pdf/OAJESS.MS.ID.000154.pdf> Accessed December 2020.
- [2] Gebel, J., and Yüce, S., 2008, *An Engineer's Guide to Desalination*, VGB PowerTech, Essen, Germany.
- [3] Abu-Zeid, M., and Shiklomanov, I. A., "Water Resources as a Challenge of the Twenty-First Century 2003," World Meteorological Organization, http://library.wmo.int/doc_num.php?explnumid=9027, Accessed January 2021.
- [4] Bond, N. R., Burrows, R. M., Kennard, M. J., and Bunn, S. E., 2019, *Multiple Stressors in River Ecosystems*, S. Sabater, A. Eloegi, and R. Ludwig, eds., Elsevier, Amsterdam, pp. 111–129.
- [5] Ruan, G., Wang, M., An, Z., Xu, G., Ge, Y., and Zhao, H., 2021, "Progress and Perspectives of Desalination in China," *Membranes*, **11**(3), p. 206.
- [6] Public Health and the Environment World Health Organization, 2007, "Guidance for the Health and Environmental Aspects Applicable to Desalination," http://www.who.int/water_sanitation_health/gdwqrevision/desalination.pdf, Accessed January 2021.
- [7] Sharqawy, M. H., Lienhard, J. H., Mistry, K. H., and Thiel, G. P., 2017, "Thermodynamics, Exergy, and Energy Efficiency in Desalination Systems," *Desalination Sustainability: A Technical, Socioeconomic, and Environmental Approach*, H. A. Arafat, ed., Elsevier, Amsterdam, pp. 1–86.
- [8] Thimmaraju, M., Sreepada, D., Babu, S., Dasari, K., Velpula, S., and Vallepu, N., 2018, "Desalination of Water," *Desalination and Water Treatment*, E. Murat, and Y. Ebubekir, eds., IntechOpen, London, UK, pp. 333–347.
- [9] Isaka, M., 2012, "Water Desalination Using Renewable Energy," International Renewable Energy Agency (IRENA), <http://www.irena.org/-/media/Files/IRENA/Agency/Publication/2012/IRENA-ETSAP-Tech-Brief-112-Water-Desalination.pdf>, Accessed December 2020.
- [10] Al-Karaghoul, A., and Kazmerski, L., 2013, "Energy Consumption and Water Production Cost of Conventional and Renewable-Energy-Powered Desalination Processes," *Renewable Sustainable Energy Rev.*, **24**, pp. 343–356.
- [11] Casimiro, S., 2015, "Concentrating Solar Power + Desalination Plants (CSP + D): Models and Performance Analysis," Ph.D. thesis, University of Lisbon, Lisbon, Portugal.
- [12] Clayton, R., 2015, "Desalination for Water Supply," Foundation for Water Research, <http://www.fwr.org/desal.pdf>, Accessed January 2021.
- [13] Brogioli, D., La Mantia, F., and Yip, N. Y., 2018, "Thermodynamic Analysis and Energy Efficiency of Thermal Desalination Processes," *Desalination*, **428**, pp. 29–39.
- [14] Askari, I., and Amerim, M., 2021, "A Techno-Economic Review of Multi Effect Desalination Systems Integrated With Different Solar Thermal Sources," *Appl. Therm. Eng.*, **185**(9), pp. 1–48.

- [15] Brika, B., 2018, "Water Resources and Desalination in Libya: A Review," *Proceedings*, **2**(11), p. 586.
- [16] Ghaffour, N., Bundschuh, J., Mahmoudi, H., and Goosen, M., 2015, "Renewable Energy-Driven Desalination Technologies: A Comprehensive Review on Challenges and Potential Applications of Integrated Systems," *Desalination*, **356**, pp. 94–114.
- [17] Al-Mutaz, I. S., 2014, "Features of Multi-Effect Evaporation Desalination Plants," *Desalin. Water Treat.*, **54**(12), pp. 3227–3235.
- [18] Salimi, M., and Amidpour, M., 2017, "Modeling, Simulation, Parametric Study and Economic Assessment of Reciprocating Internal Combustion Engine Integrated with Multi-Effect Desalination Unit," *Energy Convers. Manage.*, **48**(1), p. 138, pp. 299–311.
- [19] Cherif, H., Champenois, G., and Belhadj, J., 2016, "Environmental Life Cycle Analysis of a Water Pumping and Desalination Process Powered by Intermittent Renewable Energy Sources," *Renewable Sustainable Energy Rev.*, **59**, pp. 1504–1513.
- [20] Hatzikioseyan, A., Vidali, R., and Kousi, P., "Modelling and Thermodynamic Analysis of a Multi Effect Distillation (MED) Plant for Seawater Desalination 2003," Site Seer X, <http://citeseerx.ist.psu.edu/viewdoc/citations;jsessionid=FECABBC2FCA9CED5DC2428E4E1F353C1?doi=10.1.1.625.318>, Accessed January 2021.
- [21] Ameri, M., Mohammadi, S. S., Hosseini, M., and Seifi, M., 2009, "Effect of Design Parameters on Multi-Effect Desalination System Specifications," *Desalination*, **245**(1–3), pp. 266–283.
- [22] Abdul-Wahab, S. A., Reddy, K. V., Al-Hatmi, S. M., and Tajeldin, Y., 2011, "Development of a Steady-State Mathematical Model for Multistage Flash (MSF) Desalination Plant," *Int. J. Energy Res.*, **36**(6), pp. 710–723.
- [23] Shen, S., Zhou, S., Yang, Y., Yang, L., and Liu, X., 2011, "Study of Steam Parameters on the Performance of a TVC-MED Desalination Plant," *Desalin. Water Treat.*, **33**(1–3), pp. 300–308.
- [24] Al-Mutaz, I. S., and Wazeer, I., 2014, "Development of a Steady-State Mathematical Model for MEE-TVC Desalination Plants," *Desalination*, **351**, pp. 9–18.
- [25] Zhou, S., Gongb, L., Liua, X., and Shenb, S., 2019, "Mathematical Modeling and Performance Analysis for Multi-Effect Evaporation/Multi-Effect Evaporation with Thermal Vapor Compression Desalination System," *Appl. Therm. Eng.*, **159**, pp. 1–14.
- [26] Qi, C. H., Feng, H. J., Lv, Q.-C., Xing, Y.-L., and Li, N., 2014, "Performance Study of a Pilot-Scale Low-Temperature Multi-Effect Desalination Plant," *Appl. Energy*, **135**, pp. 415–422.
- [27] Gao, H., Jiang, A., Huang, Q., Xia, Y., Gao, F., and Wang, J., 2020, "Mode-Based Analysis and Optimal Operation of MSF Desalination System," *Processes*, **8**(7), p. 794.
- [28] Zhou, S., Shen, S., Guo, Y., and Mu, X., 2017, "Comparative Performance Evaluation of LT-MEE Desalination Systems with Three Feed Configurations," *Desalin. Water Treat.*, **69**, pp. 217–228.
- [29] Guo, P., Li, T., Li, P., Zhai, Y., and Li, J., 2020, "Study on a Novel Spray-Evaporation Multi-Effect Distillation Desalination System," *Desalination*, **473**, p. 114195.
- [30] Al-Hotmani, O. M. A., Al-Obaidi, M. A. A., John, Y. M., Patel, R., and Mujtaba, I. M., 2020, "Scope and Limitations of the Mathematical Models Developed for the Forward Feed Multi-Effect Distillation Process—A Review," *Processes*, **8**(9), p. 1174.
- [31] Liu, C., Bi, M., Zhou, Y., and Cui, G., 2020, "A Novel Model for Evaporator Structural Design in the Multi-Effect Evaporation Plant," *Appl. Therm. Eng.*, **176**, p. 115351.
- [32] Muftah, A., 2016, "Study of the Possibility to Produce Electricity From Destroyed Energy in Zuara Desalination Plant," Proceedings of 1st International Conference of Chemical and Petroleum Engineering, Alkhoms, Libya, Dec. 20–22, pp. 805–812.
- [33] El-Helw, M., El-Maghlany, M. M., and El-Ashrawy, W. M., 2020, "Novel Sea Water Desalination Unit Utilizing Solar Energy Heating System," *Alexandria Eng. J.*, **59**(2), pp. 915–924.
- [34] Muftah, A., Abugderah, M., and Dakhel, H., 2018, "Boilers Performance Evaluation of Zuara Desalination Plant," *AIJR Proc.*, **2**, pp. 290–297.
- [35] Muftah, A., and Fella, G., 2009, "Exergy Analysis for Unit Two of Zuara Desalination Plant," Proceedings of 1st International Chemical and Process Engineering Conference, Tripoli, Libya, May 5–7, Paper No. CHE-EA-01.